

Raman Spectroscopy resolution limits overcome with nanoscale thermal analysis for complete Polymer Blend Characterization

Authors: J. Ye; N. Kojima; M. Reading; K. Kjoller, R. Shetty

Introduction

Characterizing polymer blends can sometimes present a significant challenge for a single technique and the best way is a combination of techniques. In this application note, we discuss an PA6-PET blend which was initially characterized via Raman Spectroscopy at a 500nm spatial resolution. Subsequent thermal characterization at a sub-100nm spatial resolution via the nano-TA revealed a lot of interesting details and more complex sub-structures that were not available from the Raman study and helped in obtaining a detailed understanding of the blend.

nano-TA is a local thermal analysis technique which combines the high spatial resolution imaging capabilities of atomic force microscopy with the ability to obtain an understanding of the thermal behaviour of materials with a spatial resolution of sub-100nm. (a breakthrough in spatial resolution ~50x better than the state of the art). The conventional AFM tip is replaced by a special nano-TA probe that has an embedded miniature heater and is controlled by the specially designed nano-TA hardware and software. This nano-TA probe enables a surface to be visualised at nanoscale resolution with the AFM's routine imaging modes which enables the user to select the spatial locations at which they would like to investigate the thermal properties of the surface. The user then obtains this information by applying heat locally via the probe tip and measuring the thermomechanical response.

Experimental Setup

Raman microscopy was performed with a Confocal Raman system with spatial resolution of 500nm (details are proprietary to Nissan ARC). The nanoscale thermal results were obtained using a Veeco Dimension 3100 AFM equipped with an Anasys Instruments (AI) nano-thermal analysis (nano-TA) accessory and AI micro-machined thermal probe. Imaging and localised thermal analysis (LTA) spatially accurate at the 100nm scale was performed. The contact and tapping modes were used to acquire surface images and LTA employed to determine the glass transition temperature (T_g) of the different domains at a 10°C /s heating rate.

The nano-TA data presented are the cantilever deflection (while the probe is in contact with the sample surface and the feedback turned off) plotted against the probe temperature. This measurement is analogous to the well established technique of thermo-mechanical analysis (TMA) and is known as nano-TA. Events such as melting or glass transitions that result in the softening of the material beneath the tip, produce a downward deflection of the cantilever. Further information on this technique can be obtained at www.anasysinstruments.com.

Results and discussion

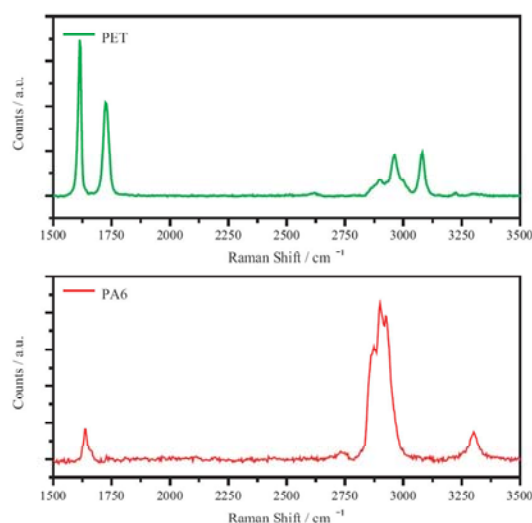


Fig 1. Raman spectra for PET and PA6

The blend of PA6 and PET investigated here was a ratio of 1:3. It was first characterized with Raman spectroscopy and nano-TA was used to further characterize the sample in regions where the spatial resolution of the Raman technique was insufficient and to obtain additional information. In figure 1, the Raman spectra for PET and PA6 are given.

Figure 2 shows Raman images of the blend at different wave numbers; on the left is the Raman

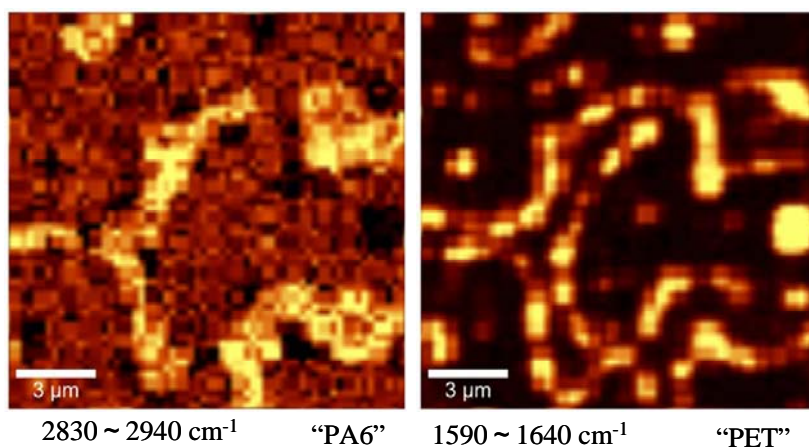


Fig 2. Raman images of the blend at the indicated wave numbers

islands of PA6 surrounded by PET with some occluded domains of PET within a matrix whose composition is not well defined.

As stated above, based on the Raman images shown in figure 2, we can see that the polymer blend has occluded regions whose central portion is composed of PA6 surrounded by a layer of

image at 2830-2940 cm^{-1} which highlights the PA6 given its dominant peak at 2900 cm^{-1} . On the right is the Raman image at 1590-1640 cm^{-1} which highlights the PET regions due to one of the dominant peaks in its spectra occurring at 1600 cm^{-1} . On the basis of this, we can identify occluded

PET. There are also domains of PET which correspond to dark areas in the 2830-2940 cm^{-1} image and so are not associated with PA6.

Information from nano-TA:

Fig 3 shows an AFM phase image of the edge of the PET region that is in contact with the PA6 as well as the inside PA6. It can be seen that there is structure in the PET regions that surround occluded PA6 domains that is of the order of tens of nanometres and thus much smaller than

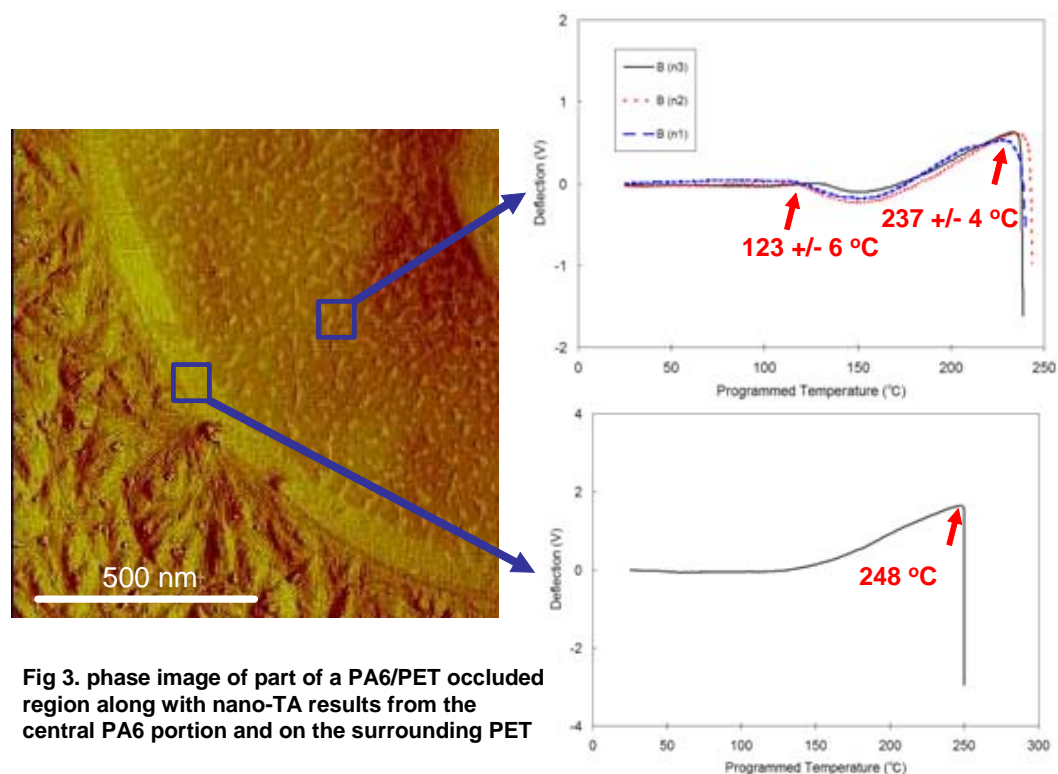


Fig 3. phase image of part of a PA6/PET occluded region along with nano-TA results from the central PA6 portion and on the surrounding PET

can be resolved with Raman microscopy. There is a border around the region which is about 100nm wide and beyond this there is another type of structure in the more central region. The

border shows a transition at 248°C which can clearly be ascribed to PET which then agrees with the Raman data. The more central PA6 region, that the Raman data shows to be PA6, exhibits a melting transition at 237 °C which is much higher than 220 °C which is the melting temperature of PA6. The curves for this region also show a transition at 123 °C which has all the characteristics of a glass transition. The T_g of PET is around 70 °C while for PA6 it is 50 °C. The rapid heating rates used in these experiments, around 20°C/sec., will give rise to a higher T_g than is seen in more conventional thermal analysis experiments but this cannot explain the greatly elevated temperature that is seen here. The most probable explanation is that this arises from the so-called rigid amorphous fraction. It is well known that amorphous regions located between crystalline domains can be made rigid by the constraints on mobility imposed by the

crystalline material and so the T_g of this material is increased. As for the higher melting temperature exhibited by the central region of PA6, we think ultra high heating rate and ultra small melting area leads, in this case, to suppression of the relief of the molecular orientation by the border around the melting area. Thus polymer chains of PA6 crystals are still in an oriented state in the melt, thereby reducing melting entropy and resulting in a higher melting point. This suggests that the melting temperature as measured by nano-TA may give us more information about polymer orientation if we apply different heating rates and this will be the subject of future work.

Figure 4 shows the AFM topography image of the matrix material between the PA6/PET domains has a clear structure with circular domains that are approximately 1-3 microns.

The Raman image at 1590-1640 cm^{-1} (which highlights the PET) does show some features of

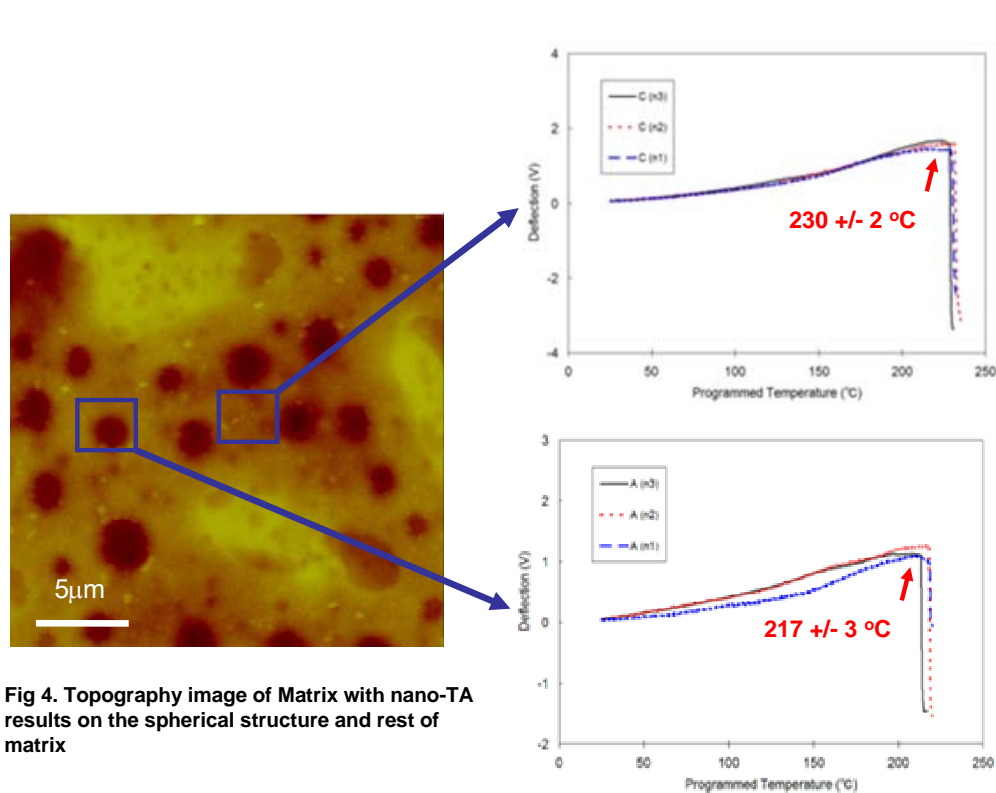


Fig 4. Topography image of Matrix with nano-TA results on the spherical structure and rest of matrix

this size that appear to be PET domains within a matrix that has a composition that must be some combination of the two materials. In figure 8 we can see that the melting temperature within the circular domains

is 217 \pm 3°C which is the melting temperature for the PA6 (within experimental error). The material between these domains has a higher melting temperature but one that is lower than the melting temperature of pure PET. High resolution AFM images of these also show clear structural differences. It can be concluded that the circular domains seen in the AFM image in figure 4 are not those seen in the Raman image that highlights PET in figure 2 both because of the low melting temperature and because they can be seen to be present at a higher density

than the PET domains figure 6 reveals. Consequently there are roughly circular domains on a scale of microns that are PET-rich and also ones that are PA6-rich. Closer inspection of the 2830-2940 cm^{-1} image (that highlights PA6) in figure 2 does suggest that there are poorly resolved micron-scale features not associated with PA6 and so this lends support to the nano-TA data.

In summary; the PA6/PET blend is a complex system and characterising its structure presents a significant challenge. There are PA6 or PA6-rich domains that are surrounded by PET or PET-rich material. The PET in these features has a substructure; there is a 100nm outer casing that is highly crystalline PET. Within the central PA6 domains there is a region that has a significant amount of amorphous material that has a very high T_g . This elevated glass transition arises because the amorphous domains have become rigid probably because of their intimate association with the crystalline phase. There is the interesting observation that the occluded PA6 domains have a higher-than-expected melting temperature and the explanation for this is the subject of on-going work. In addition to these two-phase domains, there are single phase domains of 1-3 microns of both PET-rich and PA6-rich material. Surrounding all of these is a matrix that is a mixture of PET and PA6 which has a melting temperature intermediate between these two materials.

Conclusions

AFM and nano TA can be used without other techniques to assess the structure of materials difficult to characterise by other means such as Raman microscopy. In the case investigated here excellent agreement and complementarity between the Raman and nano-TA data was achieved in determining the composition of the different domains. The different techniques provide different information, the Raman spectra can give unequivocal information on chemical composition while the AFM and nano-TA provide higher spatial resolution, and information on transition temperature that can be using to identify materials and differentiate easily between crystalline and amorphous phases. These investigations can be seen as generic examples of the general problem of characterizing the structure and composition of materials on a nano-scale and as such the range of applications is potentially vast.